

Thermodynamic phase transition of UH_3 : Role of electronic strong correlation

Yu-Juan Zhang,¹ Bao-Tian Wang,^{1,2} Yong Lu,¹ and Ping Zhang^{1,3,*}

¹*LCP, Institute of Applied Physics and Computational Mathematics, Beijing 100088, People's Republic of China*

²*Institute of Theoretical Physics and Department of Physics, Shanxi University, Taiyuan 030006, People's Republic of China*

³*Center for Applied Physics and Technology, Peking University, Beijing 100871, People's Republic of China*

The electronic structure and thermodynamical properties of uranium trihydrides ($\alpha\text{-UH}_3$ and $\beta\text{-UH}_3$) have been studied using first-principles density functional theory. We find that inclusion of strong electronic correlation is crucial in successfully depicting the electronic structure and thermodynamic phase stability of uranium hydrides. After turning on the Hubbard parameter, the uranium $5f$ states are divided into well-resolved multiplets and their metallicity is weakened by downward shift in energy, which prominently changes the hydrogen bond and its vibration frequencies in the system. Without Coulomb repulsion, the experimentally observed $\alpha \rightarrow \beta$ phase transition cannot be reproduced, whereas, by inclusion of the on-site correlation, we successfully predict a transition temperature value of about 332 K, which is close to the experimental result.

PACS numbers: 71.27.+a, 71.15.Mb, 63.20.D-

Since the report of UH_3 as one ferromagnetic (FM) uranium compounds¹⁻³, it has attracted lots of attentions in nuclear fuel field in the past decades. In solid state, uranium hydride exists mainly in the form of cubic trihydride ($\text{Pm}\bar{3}\text{n}$; No. 223)⁴ with two allotropes, i.e., $\alpha\text{-UH}_3$ and $\beta\text{-UH}_3$. $\alpha\text{-UH}_3$ [Fig. 1(a)] is an intermediate state from orthorhombic $\alpha\text{-U}$ saturated with H to $\beta\text{-UH}_3$ ⁵⁻⁷. It is the metastable low temperature phase with two UH_3 formula units in one unit cell. The uranium and hydrogen atoms in this structure occupy the 2(a) (0, 0, 0) and 6(c) ($1/4, 0, 1/2$) sites, respectively. $\beta\text{-UH}_3$ [Fig. 1(b)] is the stable high temperature phase with eight UH_3 formula units in one unit cell. The uranium atoms in this structure occupy the 2(a) (0, 0, 0) and the 6(c) ($1/4, 0, 1/2$) sites, and the hydrogen atoms occupy the 24(k) (0, 0.156, 0.313) sites. Mulford *et al.*⁶ found through X-ray diffraction measurement that the transition temperature of $\alpha\text{-UH}_3$ to $\beta\text{-UH}_3$ is between 373 K and 523 K, while Genossar *et al.*⁷ reported that $\alpha\text{-UH}_3$ transits irreversibly into $\beta\text{-UH}_3$ above room temperature. At even higher temperatures (above 673 K), uranium hydride reversibly remove the hydrogen. This property makes uranium hydrides convenient starting materials to create chemically reactive uranium powder along with various uranium carbide, nitride, and halide compounds. In contrast to the above mentioned experimental measurements on temperature-induced $\alpha \rightarrow \beta$ phase transition of uranium trihydride, to date the theoretical exploration of this prominent phase transition is still totally lacking in the literature. Considering the combined fact that (i) UH_3 denotes a typical prototype among various kinds of actinide hydrides and (ii) the actinide hydrides play extremely important role in nuclear fuel design (as well as stockpile) in which the thermodynamic stability is a substantial factor, therefore, a revealing theoretical study on the ground-state properties and $\alpha \rightarrow \beta$ phase transition of UH_3 from first-principles quantum mechanics is highly needed for the relevant important industrial applications.

From basic point of view, it can be visualized that

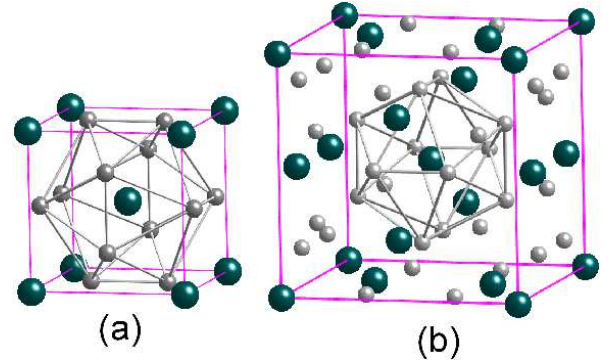


FIG. 1: (Color online) Crystal structures of (a) $\alpha\text{-UH}_3$ and (b) $\beta\text{-UH}_3$, where the large and small balls denote the uranium and hydrogen atoms, respectively.

many physical and chemical properties of UH_3 are closely related to the quantum process of localization and delocalization for partially filled uranium $5f$ electrons. Modeling of the electron localization/delocalization, and thus any hydrogenation process involving uranium, is a complex task. Conventional density functional theory (DFT) schemes that apply the local density approximation (LDA) or the generalized gradient approximation (GGA) underestimate the strong on-site Coulomb repulsion of the uranium $5f$ electrons and consequently fail to capture the correlation-driven localization. Therefore, the uranium $5f$ electrons require special attention in trying to gain any microscopic insight into the thermodynamical stability of UH_3 . Up to now several approaches, the LDA/GGA+ U , the hybrid density functional of (Heyd, Scuseria, and Enzerhof) HSE, the self-interaction corrected local spin-density (SIC-LSD), and the Dynamical Mean-Field Theory (DMFT), have been developed to correct the pure LDA/GGA failures in calculations of actinide compounds. Among these techniques, the effective modification of pure DFT by LDA/GGA+ U formalisms

has been confirmed widely in study of uranium (as well as its neighbor, plutonium) oxides^{8–10}. By tuning the effective Hubbard parameter in a reasonable range, the antiferromagnetic (AFM) Mott insulator features of these oxides were correctly calculated and the atomic structural parameters as well as the electronic properties are well in accord with experiments. Inspired by this series of successful calculations on AFM uranium oxide, as well as motivated by the fact that uranium hydride is also a magnetic ordered (FM instead of AFM) compound and thus a static mean-field treatment like LDA/GGA+ U is expected to reliably catch its some key features in both α and β phases, in the present work, we investigate the ground-state electronic properties and lattice dynamics of the two allotropes of UH_3 using the LDA+ U formalism. For comparison the pure LDA calculation is also performed. The most insightful result of our investigation is that it is essential to take the 5*f* on-site electronic correlation into account for theoretically reproducing the experimentally observed $\alpha \rightarrow \beta$ phase transition of UH_3 at finite temperature. Also, the prominent changes in the hydrogen bond and the consequent hydrogen vibration (reflected by the optical branches in phonon spectrum) in UH_3 by the inclusion of on-site Coulomb repulsion of the uranium 5*f* electrons is for the first time highlighted in this paper.

The calculations are performed using the projector-augmented wave (PAW) method of Blöchl¹¹, as implemented in the Vienna *ab initio* simulation program (VASP)¹². For the plane-wave set, a cut-off energy of 500 eV is used. The hydrogen 1*s* and uranium 6*s*²6*p*⁶6*d*²5*f*²7*s*² are treated as valence electrons. The strong on-site Coulomb repulsion amongst the localized uranium 5*f* electrons are accounted for by using the formalism formulated by Dudarev *et al.*¹³. In this scheme the total energy functional is of the form

$$E_{\text{LDA}+U} = E_{\text{LDA}} + \frac{U-J}{2} \sum_{\sigma} [\text{Tr} \rho^{\sigma} - \text{Tr} (\rho^{\sigma} \rho^{\sigma})], \quad (1)$$

where ρ^{σ} is the density matrix of *f* states, and U and J are the spherically averaged screened Coulomb energy and the exchange energy, respectively. Here the Coulomb U is treated as a variable, while the exchange energy is set to be a constant $J=0.51$ eV. This value of J is in the ball park of the commonly accepted one for uranium. Since only the difference between U and J is significant¹³, thus we will henceforth label them as one single parameter, for simplicity labeled as U_{eff} , while keeping in mind that the non-zero J has been used during calculations. The Brillouin-zone (BZ) integrations are performed using $9 \times 9 \times 9$ and $7 \times 7 \times 7$ Monkhorst-Pack¹⁴ special k -points for α - UH_3 and β - UH_3 , respectively. The geometries are optimized until the forces are less than 0.02 eV/Å, and the total energy is relaxed until the difference value is smaller than 10^{-5} eV.

Through calculating the total energy dependences on U_{eff} of α - UH_3 and β - UH_3 in nonmagnetic, FM, and AFM phases, we find that the FM phase is the most favorable

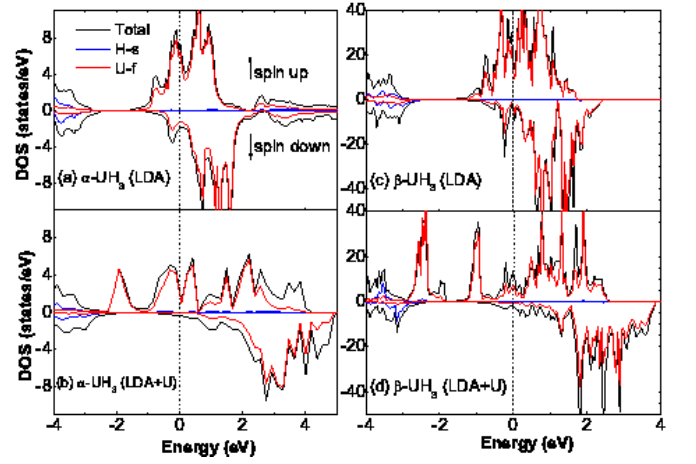


FIG. 2: (Color online) Spin-resolved total DOS for the two allotropes of UH_3 calculated within LDA and LDA+ U ($U_{\text{eff}}=4$ eV) formalisms. Partial DOS of U 5*f* and H 1*s* orbitals are also shown. The fermi level is set to be zero.

state with U_{eff} from 0 to 7 eV, which is well consistent with the experiment. The dependence of the lattice parameters on U_{eff} for FM phase of α - UH_3 and β - UH_3 demonstrates that in α phase, the lattice parameter is close to the experimental value when U_{eff} is in range of 4–6 eV, while in β phase, the range is in 4–5 eV. Considering the two allotropes, therefore, we choose the value of U_{eff} to be 4 eV in our following study for the two phases. Our calculated lattice constants for α (β) phase of UH_3 at $U_{\text{eff}}=0$ and 4 eV are 4.001 (6.382) and 4.128 (6.622) Å, respectively. Compared with pure LDA, our LDA+ U gives closer values with respect to the experimental values of 4.160⁶ and 6.639¹⁵ Å for α and β phase, respectively.

Our calculated spin-resolved total density of states (DOS) and the partial DOS for uranium 5*f* and hydrogen 1*s* states of the two allotropes are presented in Fig. 2. The upper panels show the pure LDA results, while the lower ones give the LDA+ U results. From Fig. 2 we can observe evident effects of strong correlation on the *f* states. For both two phases of UH_3 , after turning on the Hubbard U parameter, clearly, the uranium 5*f* states are divided into more well-resolved peaks compared with pure LDA, and the energy distributions of these multiple 5*f* peaks are much localized and separated. As a result of this multiple peak splitting, for α phase, the uranium 5*f* states in the range of -1.0 to 2.0 eV within LDA are extended to lie in the range of -2.5 to 5.0 eV in the LDA+ U formalism. For β phase, similar effects of strong correlation can be found. Moreover, the occupation of both spin-up and spin-down electrons at the Fermi level are lowered after taking into account the on-site Coulomb repulsion. However, no insulating band gap are opened by the inclusion of Hubbard parameter and UH_3 still remains its metallic nature as observed in the experiment¹⁶.

TABLE I: Bader effective atomic charges and volumes of α -UH₃ and β -UH₃ in the LDA and LDA+ U ($U_{\text{eff}} = 4$ eV) formalisms.

Allotrope	Methods	Q(U _I)	Q(U _{II})	Q(H)	V(U _I)	V(U _{II})	V(H)
α -UH ₃	LDA	12.527		1.490	17.913		4.703
	LDA+ U	12.425		1.525	18.847		5.415
β -UH ₃	LDA	12.503	12.434	1.503	18.290	17.465	4.904
	LDA+ U	12.452	12.370	1.535	18.774	19.283	5.706

Due to the decrease in metallicity of uranium $5f$ states and their energy downward shift towards the hydrogen $1s$ orbital by taking account of the electronic strong on-site correlation, the ionicity of the hydrogen bond is prominently enhanced. To analyze the ionicity of the two allotropes of UH₃, results from the Bader analysis¹⁷ are shown in Table I. The charge (Q) enclosed within the Bader volume (V) is a good approximation to the total electronic charge of an atom. Note that although we have included the core charge in charge density calculations, since we do not expect variations as far as the trends are concerned, only the valence charge is listed. From the results we calculated, it is seen that the ionicity of the two allotropes within LDA+ U are more evident than that within pure LDA. For α phase, the electrons transferred from each U atom to H atoms are 1.473 and 1.575 within LDA and LDA+ U formalisms, respectively. For β phase, electrons transferred from two inequivalent U atoms (U_I and U_{II}) to H atoms are 1.548 and 1.630, respectively, in LDA+ U formalism. Whereas, in LDA formalism the values are 1.497 and 1.566 respectively.

To illustrate the main point of this paper, i.e, the effect of electronic strong on-site correlation on the thermodynamic properties of UH₃, we have calculated the phonon dispersion and the Helmholtz free energy F of two allotropes with and without including Coulomb repulsion of $5f$ electrons. Phonon frequency calculations were carried out using the Hellmann-Feynman theorem and the direct method¹⁸. For α and β phases, we adopted $2 \times 2 \times 2$ supercells containing 64 and 256 atoms with $3 \times 3 \times 3$ and $1 \times 1 \times 1$ Monkhorst-Pack k -point meshes in the BZ integration, respectively. The forces induced by small displacements were calculated within VASP. The amplitude of all the displacements is 0.03 Å.

The calculated phonon curves along some high-symmetry directions in the BZ together with the phonon DOS are plotted in Fig. 3. Clearly, the effect of electronic strong correlation on phonon dispersion can be observed by comparing results from LDA and LDA+ U approaches. Compared with pure LDA calculation, the optical branches calculated within LDA+ U shift down by around 2.5 THz and 2.3 THz for α -UH₃ and β -UH₃, respectively. However, the acoustic branches have no evident changes for both phases. Due to the fact that uranium atom is much heavier than hydrogen atom, then the optical branches denote the hydrogen vibration while the

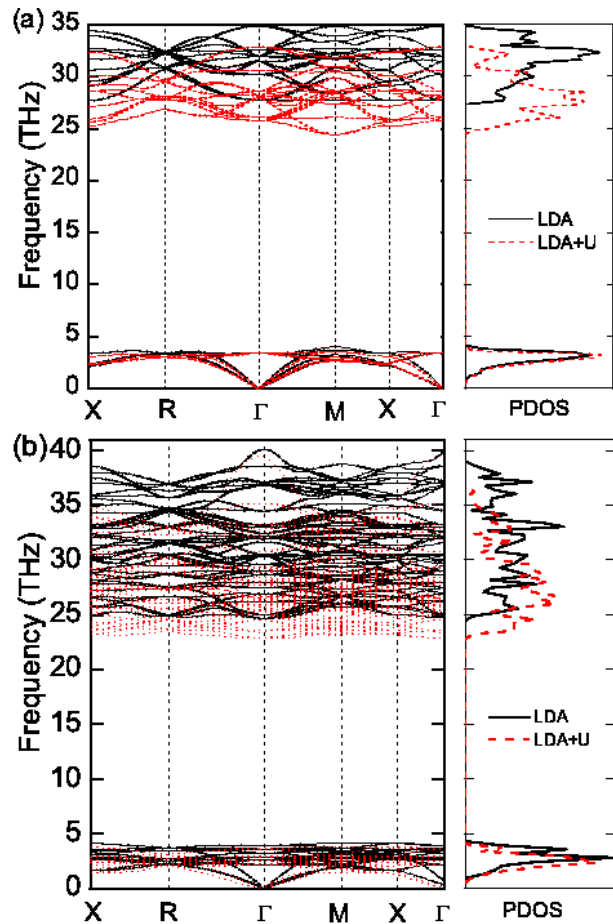


FIG. 3: (Color online) Phonon dispersion curves (left panel) and corresponding phonon DOS (right panel) of (a) α -UH₃ and (b) β -UH₃. The black curves are computed within the LDA while the red (grey) curves the LDA+ U formalism.

acoustic branches come from the uranium vibration. As a result, a large gap between optical and acoustic modes can be observed. The key point revealed in Fig. 3 is that the lattice dynamics behaviors are prominently influenced by electronic strong on-site correlation, which has changed the U-H bonding nature. This influence on lattice dynamics turns out, as analyzed below, to be fundamental to reproduce the experimentally observed relative thermodynamic stability sequence of α and β phases of UH₃.

For the sake of determining phase transition temperature of α -UH₃ and β -UH₃ at ambient condition, we have calculated the Helmholtz free energy F in the LDA and LDA+ U formalisms. This quantity at volume V and temperature T can be expressed as

$$F(V, T) = E(V) + F_{\text{vib}}(V, T) + F_{\text{ele}}(V, T), \quad (2)$$

where $E(V)$ is the 0 K band energy, $F_{\text{vib}}(V, T)$ is the phonon vibrational free energy, and F_{ele} is the thermal electronic contribution to the free energy. The phonon

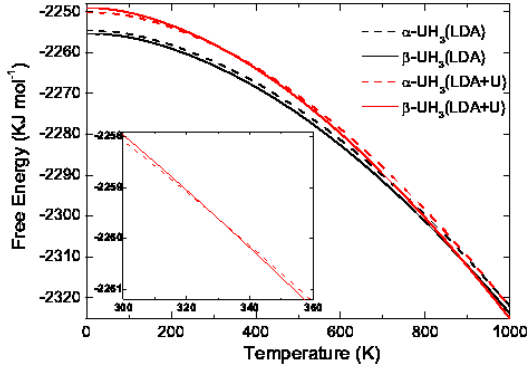


FIG. 4: (Color online) Temperature dependences of the Helmholtz free energies within LDA (the black curves) and LDA+ U (the red/grey curves) formalisms. The inset gives closer view of the crossing point within the LDA+ U .

vibrational free energy in the quasiharmonic approximation can be calculated from phonon DOS $g(\omega, V)$ as $F_{\text{vib}}(V, T) = k_B T \int_0^\infty g(\omega, V) \ln[2 \sinh(\frac{\hbar\omega}{2k_B T})] d\omega$. The thermal electronic contribution can be described as $F_{\text{ele}}(V, T) = E_{\text{ele}} - T S_{\text{ele}}$ with electronic entropy $S_{\text{ele}}(V, T) = -k_B \int n(\epsilon, V) [f \ln f + (1-f) \ln(1-f)] d\epsilon$, where f is Fermi-Dirac distribution and n is the electronic DOS. The chemical potential at temperature T is fixed by conservation of total valence electron number during thermal excitation. It turns out that the value of the thermal electronic contribution is very small, only one-tenth of the phonon vibrational free energy.

We have calculated and plotted the temperature dependences of the Helmholtz free energy for the two UH₃ phases within LDA and LDA+ U formalisms (Fig. 4). A significant difference can be clearly observed between the two formalisms. Without including the on-site Coulomb interaction, the Helmholtz free energies of two UH₃ phases have no crossing point, and the α phase is always more thermodynamically stable than the β phase in a wide

temperature range of 0 to 1000 K, as shown in Fig. 4. This is contrary to the experimental observations. Whereas, after including the electronic strong correlation, the calculated Helmholtz free energy curves of the two allotropes cross at the temperature of 332 K, which is well consistent with the experimental value for $\alpha \rightarrow \beta$ phase transition. Therefore, we arrive at that while the pure LDA calculation totally fails to reproduce the experimentally determined thermodynamic phase transition of UH₃, the LDA+ U calculation can well depict it. This is a good news for the science of actinide hydrides. Needless to say, more advanced many-body techniques, such as DMFT, which can account for some spin fluctuations at finite temperatures, will further improve the calculations and we would like to leave it for future consideration.

In conclusion, the ground-state properties of two allotropes of UH₃ have been comparatively studied within the LDA and LDA+ U formalisms. After switching on the on-site Coulomb interaction, the uranium 5*f* states split into the multiple well-resolved peaks that shift upward or downward with respect to the Fermi energy, which reduces the metallicity of the 5*f* states and enhances the ionicity of the hydrogen bond in the system. As a result, the calculated optical branches in the phonon dispersion of two allotropes have been found to shift down by about 2.5 and 2.3 THz for α -UH₃ and β -UH₃, respectively, by turning on the Hubbard parameter. Our theoretical Helmholtz free energy curves have shown that while the pure LDA fails to describe the $\alpha \rightarrow \beta$ phase transition, the LDA+ U calculation gives the transition temperature of 332 K, which well lies within the experimentally observed range. These results clearly indicate that the electronic strong on-site correlation plays an important role in the uranium hydride systems.

This work was supported by NSFC under Grant No. 51071032, by the Foundation for Development of Science and Technology of China Academy of Engineering Physics under Grant No. 2009A0102005, and by the National Basic Security Research Program of China.

* Author to whom correspondence should be addressed. E-mail: zhang_ping@iapcm.ac.cn

- ¹ W. Trzebiatowski, A. Sliwa, and B. Stalinski, *Rocz. Chem.* **28**, 12 (1954).
- ² W. Trzebiatowski and P.W. Selwood, *J. Am. Chem. Soc.* **72**, 4504 (1950).
- ³ R. Troć and W. Suski, *J. Alloys Compd.* **219**, 1 (1995).
- ⁴ K. Balasubramanian, W.J. Siekhaus, and W. Mclean, *J. Chem. Phys.* **119**, 5889 (2003).
- ⁵ C.D. Taylor, T. Lookman, and R.S. Lillard, *Acta Mater.* **58**, 1045 (2010).
- ⁶ R.N.R. Mulford, F.H. Ellinger, and W.H. Zachariasen, *J. Am. Chem. Soc.* **76**, 297 (1954).
- ⁷ J.G. Genossar, M. Kuznitz, and B. Meerovici, *Phys. Rev. B* **1**, 1958 (1970).
- ⁸ S. L. Dudarev, D. N. Manh, and A. P. Sutton, *Philos. Mag. B* **75**, 613 (1997).

- ⁹ B. Sun, P. Zhang, and X.-G. Zhao, *J. Chem. Phys.* **128**, 084705 (2008).
- ¹⁰ P. Zhang, B.-T. Wang, and X.-G. Zhao, *Phys. Rev. B* **82**, 144110 (2010).
- ¹¹ P.E. Blöchl, *Phys. Rev. B* **50** 17953 (1994).
- ¹² G. Kresse and J. Furthmüller, *Phys. Rev. B* **54**, 11169 (1996).
- ¹³ S.L. Dudarev, G.A. Botton, S.Y. Savrasov, C.J. Humphreys, and A.P. Sutton, *Phys. Rev. B* **57**, 1505 (1998).
- ¹⁴ H.J. Monkhorst and J.D. Pack, *Phys. Rev. B* **13** 5188 (1976).
- ¹⁵ R.E. Rundle, *J. Am. Chem. Soc.* **69**, 1719 (1947).
- ¹⁶ T. Gouder, R. Eloirdi, F. Wastin, E. Colineau, J. Rebizant, D. Kolberg, and F. Huber, *Phys. Rev. B* **70**, 235108 (2004).

- ¹⁷ R. F. W. Bader, *Atoms in Molecules: A Quantum Theory* (Oxford University Press, New York, 1990). 4063 (1997).
- ¹⁸ K. Parlinski, Z.Q. Li, Y. Kawazone, *Phys. Rev. Lett.* **78**,